 doi: 10.1111/1365-2478.12157

Joint inversion of long-offset and central-loop transient electromagnetic data: Application to a mud volcano exploration in Perekishkul, Azerbaijan

A. Haroon[1]*, J. Adrian[1], R. Bergers[1], M. Gurk[1], B. Tezkan[1], A. L. Mammadov[2] and A. G. Novruzov[2]

[1]*Institute for Geophysics and Meteorology, University of Cologne, 50969, Cologne, Germany, and* [2]*Department of Seismology and Physics of Earth, Baku State University, 370145, Baku, Azerbaijan*

Received April 2013, revision accepted January 2014

ABSTRACT

Mud volcanism is commonly observed in Azerbaijan and the surrounding South Caspian Basin. This natural phenomenon is very similar to magmatic volcanoes but differs in one considerable aspect: Magmatic volcanoes are generally the result of ascending molten rock within the Earth's crust, whereas mud volcanoes are characterised by expelling mixtures of water, mud, and gas. The majority of mud volcanoes have been observed on ocean floors or in deep sedimentary basins, such as those found in Azerbaijan. Furthermore, their occurrences in Azerbaijan are generally closely associated with hydrocarbon reservoirs and are therefore of immense economic and geological interest. The broadside long-offset transient electromagnetic method and the central-loop transient electromagnetic method were applied to study the inner structure of such mud volcanoes and to determine the depth of a resistive geological formation that is predicted to contain the majority of the hydrocarbon reservoirs in the survey area. One-dimensional joint inversion of central-loop and long-offset transient electromagnetic data was performed using the inversion schemes of Occam and Marquardt. By using the joint inversion models, a subsurface resistivity structure ranging from the surface to a depth of approximately 7 km was determined. Along a profile running perpendicular to the assumed strike direction, lateral resistivity variations could only be determined in the shallow depth range using the transient electromagnetic data. An attempt to resolve further two-dimensional/three-dimensional resistivity structures, representing possible mud migration paths at large depths using the long-offset transient electromagnetic data, failed. Moreover, the joint inversion models led to ambiguous results regarding the depth and resistivity of the hydrocarbon target formation due to poor resolution at great depths (>5 km). Thus, 1D/2D modelling studies were subsequently performed to investigate the influence of the resistive terminating half-space on the measured long-offset transient electromagnetic data.

The 1D joint inversion models were utilised as starting models for both the 1D and 2D modelling studies. The results tend to show that a resistive terminating half-space, implying the presence of the target formation, is the favourable geological setting. Furthermore, the 2D modelling study aimed to fit all measured long-offset transient

*E-mail: haroon@geo.uni-koeln.de

electromagnetic Ex transients along the profile simultaneously. Consequently, 3125 2D forward calculations were necessary to determine the best-fit resistivity model. The results are consistent with the 1D inversion, indicating that the data are best described by a resistive terminating half-space, although the resistivity and depth cannot be determined clearly.

Key words: Transient electromagnetics, Joint inversion, 1D/2D modelling.

INTRODUCTION

Mud volcanism is a commonly observed natural phenomenon in Azerbaijan and the surrounding South Caspian Basin (SCB). According to Planke *et al.* (2003), over 400 active mud volcanoes have been observed within the SCB, making it the region with the highest mud volcano density in the world (Feyzullayev, Kadirov, and Aliyev 2005). Worldwide, Milkov (2000) estimates the total number of known and inferred mud volcanoes to be $10^3 - 10^5$, most of which are located in deep sea regions.

Generally, mud volcanoes differ in size, appearance, eruption intensity, and eruption characteristics (Bohrmann, Kopf, and Spiess 2006; Milkov 2000, 2005; Feyzullayev *et al.* 2005). Some appear as truncated cones rising several hundred meters above the background landscape; others are rather flat and consist of large pools. Similar to magmatic volcanoes, the appearance of mud volcanoes largely depends on eruption frequency and the characteristics of discharge. Generally, mud volcanoes are categorised into three groups based on their eruption characteristics, each group being named after a particular individual (Judd 2005a).

- Lokbatan type: Eruptions are often brief and infrequent but explosive. Expelled methane gas may self-ignite, causing a high flame above the crater.
- Chikishlyar type: The activity is generally continuous and gentle; explosive eruptions do not occur.
- Shugin type: The mass discharge is characterised by continuous activity that is interrupted by brief eruptive phases.

In recent years, mud volcanoes in Azerbaijan have attained growing economic interest as their occurrences are associated with hydrocarbon reservoirs (Bohrmann *et al.* 2006). As a consequence, the inner structure of mud volcanoes, related to both basin structure and hydrocarbon reservoir occurrence, has been explored quite frequently in recent years (e.g.; Abrams and Narimanov (1997), Stewart and Davies (2006), and Bonini *et al.* (2013)). However, most of the information is solely based on seismic or geologic data. A subsurface resistivity model of a mud volcano up to a depth of 7 km is, according to our knowledge, non-existent.

Few attempts have been made to derive shallow fluid migration paths of mud volcanoes in Azerbaijan utilising the direct current resistivity method (Scholte 2005). Moreover, several electromagnetic (EM) applications have been performed worldwide studying different mud volcano occurrences (Chow, Chang, and Yu 2006, Ellis *et al.* 2008; Istadi *et al.* 2009; Lin and Jeng 2010). A novel offshore transient controlled source EM system consisting of two transmitter polarisations has recently been applied to investigate a sea-floor mud volcano in the Mediterranean Sea (Swidinsky, Hölz, and Jegen 2013).

Within the framework of the ELMUD project ("Electromagnetic methods to study the inner structure of mud volcanoes in Perekishkul, Azerbaijan") conducted by the Institute for Geophysics and Meteorology at the University of Cologne (IGM Cologne) between 2010 and 2012, the radiomagnetotelluric (RMT), central-loop transient EM (TEM), and long-offset transient EM (LOTEM) methods were applied in Azerbaijan to study the inner structures of mud volcanoes at various depth intervals. Although the RMT method was effective in resolving small-scale resistivity variations at shallow depths in the vicinity of the investigated mud volcanoes (not shown in this publication), the general resistivity models between TEM and RMT did not differ significantly for depths smaller than 10 m. Therefore, the following investigation is confined only to the joint interpretation of TEM and LOTEM.

The study aims at resolving both shallow and deep fluid migration paths presumed to cause two-dimensional (2D)/three dimensional (3D) resistivity structures. Furthermore, the application of the LOTEM method aims to determine the depth of a resistive target formation, which, according to Abrams and Narimanov (1997) contains the majority of hydrocarbon reservoirs in the region. In order to reach the required investigation depth of at least 4 km, uncommon

acquisition times of up to 15 seconds were applied during the LOTEM measurements. This novelty in acquisition was primarily necessary due to the very low resistivities within the survey area that are comparable to the resistivities found within in the marine environment.

APPLIED ELECTROMAGNETIC METHODS

TEM is an active EM method used to resolve the shallow electrical resistivity distribution of the subsurface (Ward and Hohmann 1988; Nabighian and Macnae 1991). A schematic field setup of the central-loop configuration is displayed in Fig. 1(a). A direct current flows through a horizontal loop that is assembled on the surface of the Earth. By abruptly interrupting the current signal, EM eddy currents are generated in the subsurface that diffuse in a form corresponding to the smoke ring process (Nabighian and Macnae 1991). These currents induce a further secondary magnetic field that can be measured as induced voltage by a horizontal receiver coil located at the center of the transmitter loop. The transient behaviour of the measured signal is thereby directly related to the subsurface resistivity distribution.

In Azerbaijan, a 50 x 50 m^2 transmitter loop and a 20 x 20 m^2 receiver loop were used. The induced voltage was measured in the time range from 0.7 μs to 2 ms with a transmitter current amplitude of 1.5 A and from 40 μs to 6 ms with a transmitter current amplitude of 9.5 A corresponding to the NanoTEM and ZeroTEM modes of the Zonge transmitter-receiver system, respectively. The TEM measurements were carried out with the NT-20 transmitter and the GDP-32II receiver from Zonge Engineering.

The LOTEM method has previously been applied in hydrocarbon and geothermal exploration (Kaufman and Keller 1983), coal exploration (Stephan, Schniggenfitting, and Strack 1991), volcanic research (Müller, Hördt, and Neubauer 2002), and groundwater research (Lippert *et al.* 2012). A schematic LOTEM field setup of the broadside configuration applied in Azerbaijan is displayed in Fig. 1(b). For this setting, the receivers are installed alongside the transmitter at a distance referred to as the offset.

A square-wave current signal (Fig. 1(c)) with an amplitude of 30–35 A and a period of 24 seconds or 30 seconds was injected using the GGT-30 transmitter (Zonge Engineering) over a dipole with a length of 750 m and 850 m. At an offset of 4-8 km the electric and magnetic receivers (SUMMIT-USB and KMS820 acquisition units) were positioned. The potential difference caused by the horizontal electric field component in the x-direction was measured by an electric dipole using non-polarisable electrodes (see Fig. 1(d)). The vertical magnetic field component was obtained by measuring the induced voltage of a 40 m x 40 m x 54 winding receiver coil. It should be mentioned that, for LOTEM soundings, the direction of the transmitter dipole is generally defined as the x-direction.

The TEM and LOTEM methods have been applied jointly in numerous cases by the IGM Cologne to solve various geophysical problems (Scholl 2005; Lange 2003). The advantage of jointly applying the TEM and LOTEM methods is that a resistivity model can be determined corresponding to a depth range that is not resolved by the individual interpretation of each method. Thereby, the TEM transients determine the shallow resistivity structures, whereas the LOTEM transients resolve the deeper lying resistivity structures.

SURVEY AREA

The field surveys were conducted in the Azeri region of Perekishkul, located approximately 45 km northwest of the capital city Baku (Fig. 2(a)). The survey area marks the northwestern boundary of the SCB commonly referred to as the Kura Basin. This sedimentary basin is bounded to the north by the Greater Caucasus mountains and is of particular interest due to the vast occurrences of Chikishlyar mud volcanoes.

In general, the SCB is one of the deepest sedimentary basins in the world, consisting of a more than 20-km-thick sedimentary fill ranging from Mesozoic to Cenozoic (Brunet *et al.* 2002). A large portion of the sedimentary deposition occurred in a short Pliocene–Quaternary interval where the sedimentation rate within the SCB was of a factor five times higher compared with similar basins around the world (Lerche *et al.* 1996). The resulting excessive fluid pressure within the basin, in combination with tectonic overpressure, density inversion, and gas-hydrate dissociation, is the key factor leading to the formation of mud volcanoes in the region (Bohrmann *et al.* 2006; Milkov 2000, 2005; Feyzullayev *et al.* 2005).

Consequently, mud volcanism is a commonly found natural phenomenon in Azerbaijan. Approximately 300 of the 2000 mud volcano observations in the world were made in Azerbaijan (Judd 2005b). Until present, the deep subsurface resistivity structure of these mud volcanoes has not been investigated. Seismic data have been obtained at large mud volcanoes (e.g. Stewart and Davies 2006; Bonini *et al.* 2013) but is not available for the investigated survey area. However, based on these results, it is presumed that the mud origin layer may lie as deep as 14 km (Planke *et al.* 2003). As it rises to the surface, the mud passes through several different geological horizons and picks up different materials (Scholte 2005). Also, due

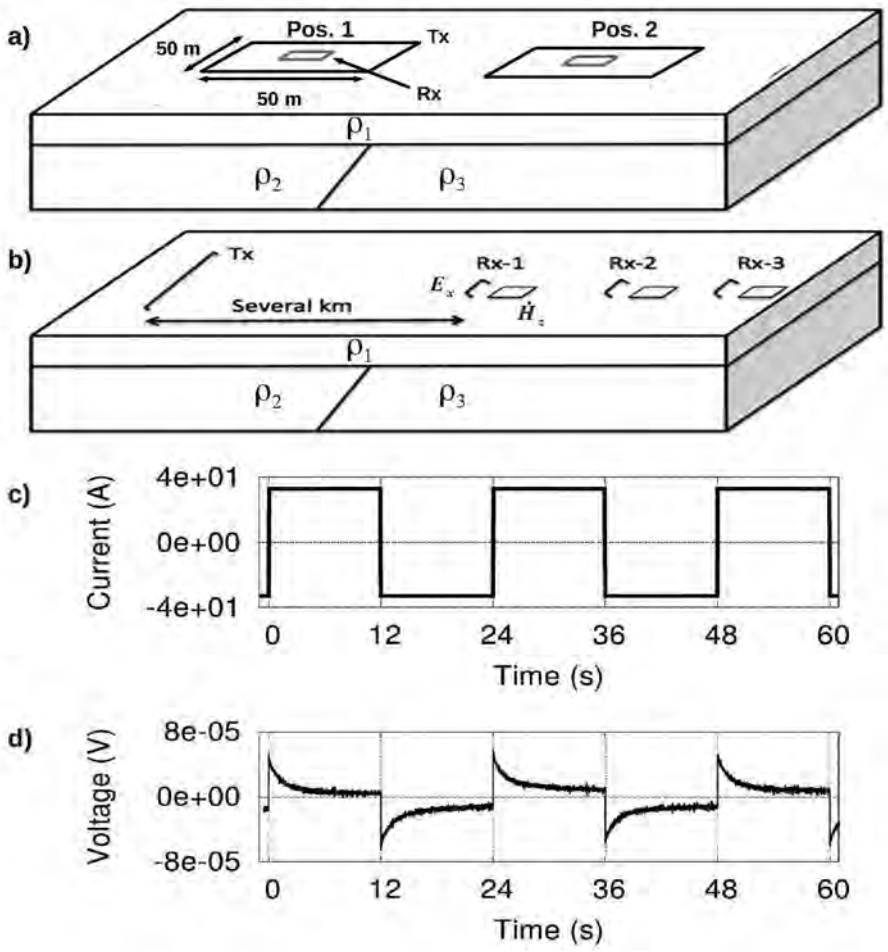

Figure 1 Schematic sketch of the central-loop TEM (a) and the LOTEM Broadside (b) field setup applied in this survey. For LOTEM, the E_x and H_z components were measured. Additionally, the LOTEM current signal (c) and LOTEM Ex receiver signal (d) are displayed for a current signal of 35 A and a period of 24 seconds.

to the common occurrence with hydrocarbon fields, mud volcanoes may often provide important channels for petroleum migration (Planke *et al.* 2003). The occurrences of hydrocarbon reservoirs are therefore often assumed based on the composition of the expelled mud volcano breccia, which consists of a mixed semi-liquid clay mass with various lithology of solid rocks derived from different age stratigraphic horizons that occur at various depths (Aliyev, Guliyev, and Rahmanov 2009). The expelled mud may also contain traces of oil or, in some cases, may pour out a lot of oil, e.g., at the Uchtape mud volcano (Aliyev *et al.* 2009). Generally, the mud rises along fault structures or in the form of a mud plume resulting in 2D/3D resistivity structures. The application of the LOTEM method aims to detect these deep-lying resistivity variations.

The EM survey investigated three different mud volcanoes named Volcano 1, Volcano 2, and Volcano 3, distributed along a line running northwest to southeast within the survey area (Fig. 2(b)). The assumption that these mud volcanoes are likely to be connected by some sort of 2D/3D resistivity structure, i.e., fault structure or mud plume, seems quite reasonable. Unfortunately, due to the high logistical expenditure, only Volcano 3 was investigated using the LOTEM method, whereas all three mud volcanoes were investigated using TEM. The following interpretation will therefore focus only on Volcano 3. It is the southernmost of the three mud volcanoes, located approximately 1 km south of the highway (see Fig. 2(b)). Figure 3 shows the crater field of the investigated volcano, which consists of several micro formations (vents) that recurrently release mud, gas, water, and traces of oil.

Figure 2 displays the field setup applied during the LOTEM field survey. In total, thousands of time series were

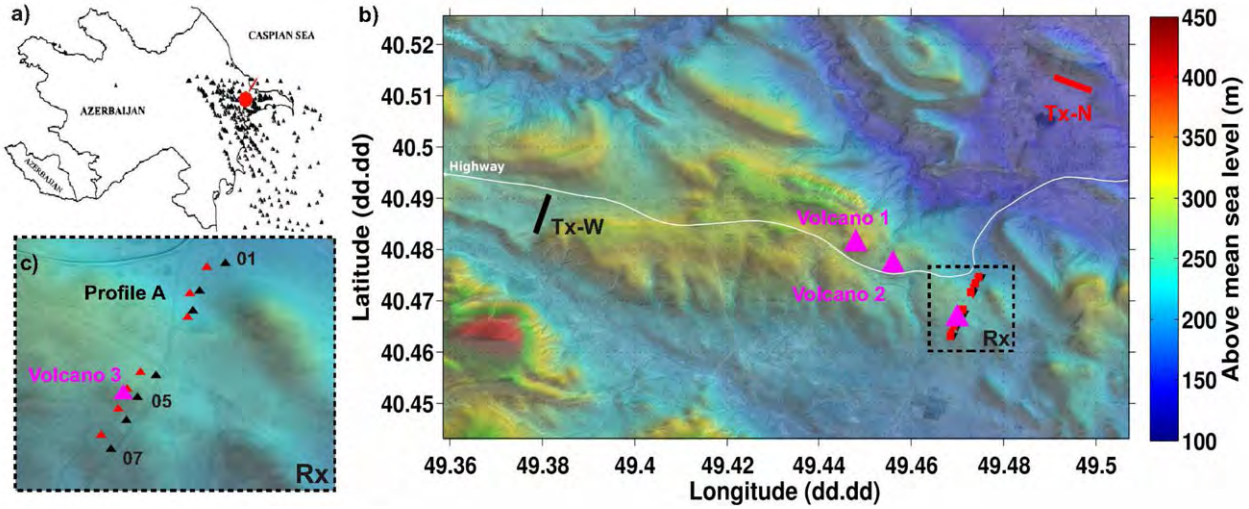

Figure 2 (a) The distribution of observed mud volcanoes onshore and offshore Azerbaijan and the location of the survey area marked by a red dot (modified after Feyzullayev et al. (2005)). (b) Topographic overlay map of the survey area, transmitter/receiver location, and position of the three mud volcanoes. The colour scale expresses the topographic data above mean sea level obtained from Jarvis *et al.*, 2008. The LOTEM transmitter and receiver locations shown in (c) are colour coded, i.e. corresponding transmitter and receiver locations have the same colour. The TEM stations are not displayed in this image but are consistent with the corresponding LOTEM stations. The map is from GoogleEarth.

recorded at 14 stations along Profile A displayed in Fig. 2(c) by the red and black markers. The profile extends from northeast to southwest, directly crossing Volcano 3 at station 05. In total, Profile A consists of 7 Ex and 7 Hz receiver stations measured from both the northern (Tx-N) and western (Tx-W) transmitter positions. In Fig. 2, the receivers are colour coded with their corresponding transmitter. The locations of the TEM stations are not explicitly shown but are generally consistent with the LOTEM receiver stations.

The perpendicular transmitter positions, one in the north and the other in the west, were chosen to investigate a possible 2D/3D resistivity structure, i.e., fault structure, mud plume, etc. within the study area. The goal is to analyse possible differences in the resulting inversion models obtained at one station from the two perpendicular transmitter positions. A strong discrepancy would indicate a 2D or even 3D resistivity distribution within the study area. In contrast, identical or fairly similar models would rather imply that the subsurface resistivity distribution varies only with the depth.

It should be mentioned that a second profile consisting of 4 Ex and 4 Hz receiver stations was measured approximately 400 m to the west of the mud volcano. The resulting inversion models are consistent with those obtained in Profile A. Therefore, the results of the second profile are not considered in this publication.

DATA PROCESSING

Measured EM time series are often contaminated by EM noise and consequently suffer from poor signal-to-noise ratios. Periodic noise generally contributes the main portion. A familiar cause is the local power network (50 Hz and harmonics). Additionally, sporadic noise sources may often appear in form of white noise, spikes, steps or drifts. It is crucial that the measured time series are processed prior to inversion to avoid misinterpretating the data.

The processing steps generally depend on the acquisition characteristics of the devices and, as a result, differ between the applied EM methods. In the following, the different processing steps of TEM and LOTEM are summarised.

Data Processing: TEM

The processing steps of the acquired TEM data sets largely depend on the measurement procedure. In the applied case, two NanoTEM transients (high and low gain) and one ZeroTEM transient were measured at each station. Each NanoTEM transient was obtained by a stacking algorithm that used 20 blocks consisting of 1024 measurements. For the ZeroTEM mode, 20 blocks consisting of 512 measurements were stacked. The goal of the data processing is to incorporate all the obtained data in the subsequent interpretation.

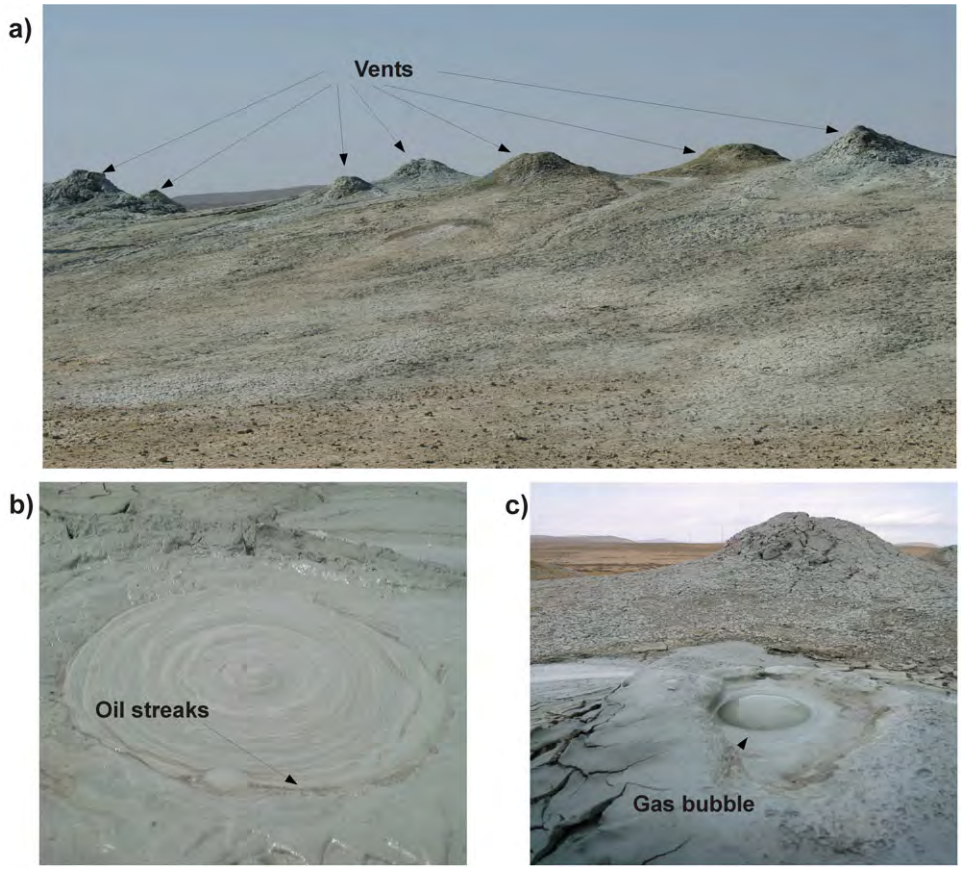

Figure 3 Pictures of the investigated mud volcano in Perekishkul, Azerbaijan. The mud volcano consists of several vents (a). Oil streaks (b) and gas (c) can be observed within the expelled mud breccia.

At this point, different strategies may be applied to handle the obtained transients. Theoretically, a joint inversion of all transients should lead to a sufficient result. However, to minimise the required computational effort, we propose to merge the NanoTEM and ZeroTEM transients to one, ideally ranging from 0.7 μs to 6 ms (Fig. 4). Before this can occur, the non-zero transmitter turn-off time (3.5μs for NanoTEM and 55μs for ZeroTEM) is removed from each transient by approximating the turn-off time as a linear ramp and by applying a deconvolution algorithm (Fitterman and Anderson 1987; Helwig, Lange, and Hanstein 2003). Subsequently, the transients are merged and overlapping time points are eliminated.

Data Processing: LOTEM

The receiver devices utilised for LOTEM data acquisition do not have an internal processing/stacking algorithm. Data processing is performed subsequent to the measurement.

Generally, the high amplitude and uniformity of the periodic noise cause the most evident contamination of the measured LOTEM signal. Typically, the periodic 50-Hz frequency and its harmonics caused by the local power network were the greatest disturbance in the measured Azerbaijan data. As demonstrated in Fig. 5(b), these periodic distortions are removed from the measured time series by applying digital filtering techniques (Hanstein 1996). The applied filters are based on the assumption that a known periodic noise frequency can be reproduced using Fourier series and subsequently subtracted from the time series. Amplitude and frequency fluctuations of the periodic noise signal are considered by filtering in predefined segments.

After filtering, the resulting time series still contain a certain number of current switches, depending on the acquisition unit (e.g., two current switches at 0 seconds and 15 seconds in Fig. 5(b)). Ultimately, the goal is to obtain one transient (one current switch-on signal). Thus, each filtered time series is cut into the number of contained current switches and

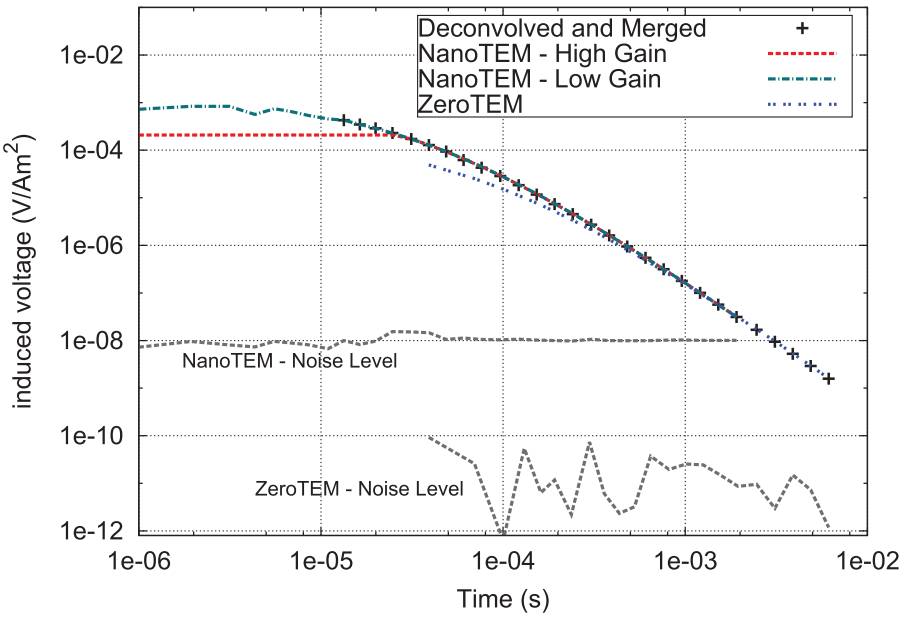

Figure 4 Merging process of TEM transients acquired at Profile A, station 01 with the NanoTEM and ZeroTEM modes in Azerbaijan. The red, turquoise and blue lines represent each of the individual Nano/Zero TEM transients and the black markers the final merged transient. Due to technical issues, the very early times (t < 1e-05 s) of the NanoTEM Low-Gain transient could not be used. The EM noise level measured for each mode is displayed by dashed-grey lines.

processed accordingly to multiply the total number of time series for later stacking purposes. Specific acquisition characteristics of the devices require a pre-trigger (also called onset) of 128 data points. Therefore, the cut is made 128 data points before each current switch, and consequently, each transient is reduced by the length (dt) depending on the sampling rate (dt = 128· sampling rate). The time series are mirrored at the x-axis and shifted along the time axis so that all time series have identical polarisation and the current switch begins at 0 seconds. Subsequently, all time series are levelled to the onset (t < 0 seconds) to simulate a switch-on current signal and selectively stacked (Fig. 5(c)) to remove sporadic noise distortions. A time-variable Hanning window (low-pass filter) is additionally applied to the resulting transients to remove the remaining noise (Fig. 5(d)).

Unfortunately, these standard processing steps could not be applied to the measured Hz transients. Additional noise sources, presumably caused by receiver coil motion due to strong winds during the measurements, prevented an interpretation of these transients. They could not be processed sufficiently using the above-mentioned steps. As a consequence, the following interpretation is solely based on the measured Ex transients.

1D INVERSION

The first step in interpreting transient EM data is often one-dimensional (1D) inversion, where the resistivity of the model is solely a function of depth ($\rho = \rho(z)$). The resulting models offer a preliminary understanding of the subsurface resistivity distribution and often provide a sufficient approximation of the true resistivity structure (Hördt *et al.* 1992).

Applied Inversion Strategy

At the surface of an arbitrary horizontally layered half-space, the EM field components generated by a loop source (TEM) or a dipole source (LOTEM) can be recursively calculated (Nabighian and Macnae 1991; Strack 1992). Different inversion algorithms can then be applied to obtain a model providing a decent fitting between measured and calculated data. The quality of fitting is thereby determined through the root-mean-square error defined as:

$$\mathrm{RMS} = \sqrt{\frac{1}{N}\sum_{i=1}^{N}\frac{(d_{i,meas} - d_{i,calc})^2}{d_{i,meas}^2}} * 100, \qquad (1)$$

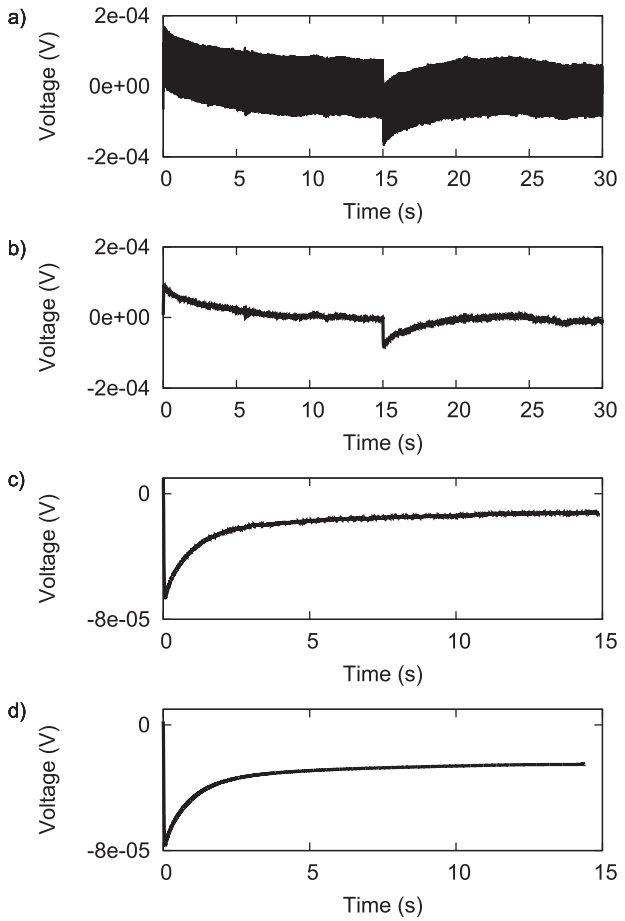

Figure 5 Chronological illustration of the LOTEM processing steps from the measured time series (a) to the processed transient (d). The raw time series (a) are superimposed by the periodic noise frequencies of 50 Hz and harmonics. These are filtered between steps a) and b) using digital filtering techniques. Subsequently, the time series are cut 128 data points before the current switch (located at 0 s and 15 s), shifted, levelled, and selectively stacked (c). Finally, the transient is smoothened with a time-variable Hanning window (d) and levelled to the onset.

where N represents the total number of data points, $d_{i,meas}$ represents the ith point of the measured data, and $d_{i,calc}$ represents the ith point of the calculated data.

In the applied 1D inversion process, two different inversion algorithms were utilised to obtain the best-fit resistivity model: damped least squares (Marquardt 1963) and Occam's smoothness constraint inversion (Constable, Parker, and Constable 1987). Furthermore, a hybrid global/deterministic approach was used to obtain equivalent models providing a qualitative interpretation of model parameter resolution (Scholl 2005).

In addition to the usual inversion parameters, layer thickness, and layer resistivity, one further parameter, called the calibration factor (CF), is often needed to fit the measured to the calculated data. Hördt (1989) and Hördt and Scholl (2004) show that shallow geological structures underneath the receivers may distort the measured LOTEM signal. These shallow structures result in a shift of the whole transient to higher or lower voltages. Additionally, receiver misalignment, improper definition of gain, receiver area, topography, current offsets, etc., may also produce this effect (Strack 1992).

The CF is a scalar value that is multiplied to the synthetic data to provide acceptable fitting between measured and calculated data. Newman (1989) concluded that this scaling allows an accurate interpretation of the deeper geological structures. However, near-surface layering will be interpreted incorrectly. Therefore, it is desired to fit the data with a CF close to 1. The data are then solely explained by layer resistivity and layer thickness, making the interpretation less ambiguous.

The acquired TEM and LOTEM transients are generally interpreted individually using the 1D inversion approach described above. However, one might also use a joint inversion approach to interpret both data sets simultaneously. The process of joint inversion for geophysical prospecting is explained by Jupp and Vozoff (1975a). The idea is to fit data of different geophysical methods to a single resistivity model. This is accomplished by combining the Jacobians into one matrix and the data vector and model functions into individual vectors while keeping the same parameter vector to fit the data. The inversion process stays consistent with the single inversion. However, it should be noted that the forward calculations have to be done separately for each EM method. The combination of both methods generally yields more satisfactory results than either TEM or LOTEM does alone. Additionally, the ambiguity of the inversion result is improved since the number of equivalent models is restricted (Jupp and Vozoff 1975a).

1D Inversion Results

The TEM and LOTEM data were individually interpreted using the 1D inversion schemes described above. A full interpretation of the individual 1D inversion models is not conducted in the extent of this publication since the results are fairly similar to the 1D joint inversion. An example is shown in Fig. 6, where a comparison between the individual TEM/LOTEM inversion models (black and blue, respectively) and the joint inversion model (red) obtained at station 01 is

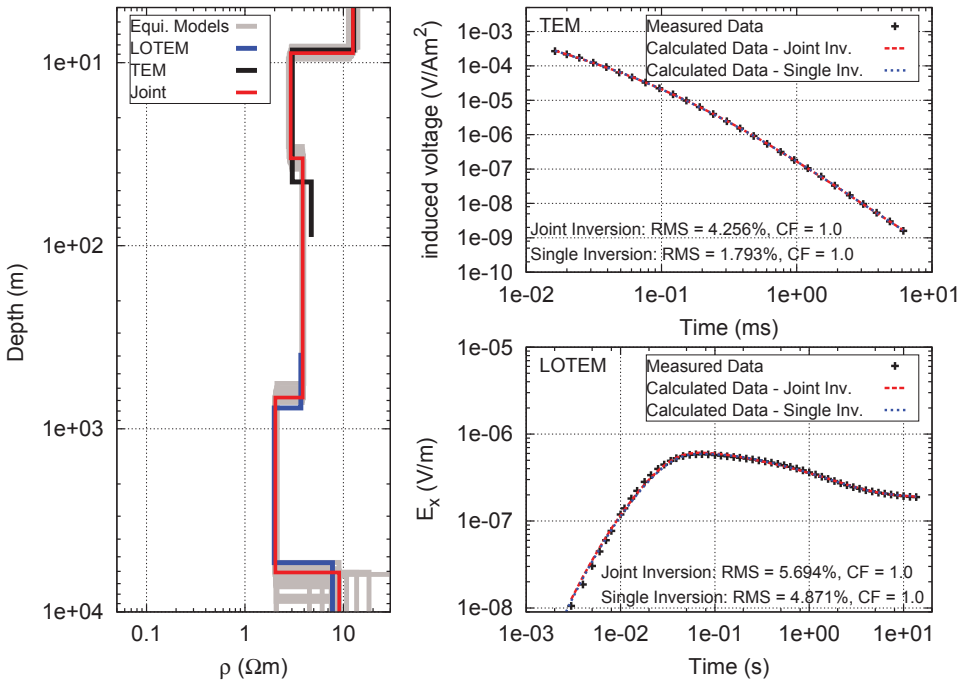

Figure 6 Comparison between TEM and LOTEM single Marquardt inversion models (solid-black and solid-blue lines, respectively) and Marquardt joint inversion model (red) at Profile A station 01. The equivalent models of the joint inversion are displayed in grey. For both TEM and LOTEM, the data fitting is displayed on the right.

displayed. The models are comparable, even though the data fitting of the individual inversion is superior compared with the joint inversion, especially for the TEM transient. However, aside from the upper boundary and resistivity of the third layer (regarding the joint inversion model) at a depth range of 30–800 m, both the joint and individual inversion models suggest a fairly similar subsurface resistivity distribution, at least within the variability of the equivalent models (grey). This behaviour is also valid for the remaining stations.

The 1D joint inversion model shown in Fig. 6 is typical for the data obtained in the survey area. Due to the scarce information available for the survey area, the following interpretation is solely based on the resistivity and thickness values provided by the 1D joint inversion and is not correlated with additional borehole data. The subsurface is generally explained by a five-layer model with resistivities ranging between 1 Ωm and 10 Ωm. The surface layer is most resistive (4 Ωm and 10 Ωm) with a variable thickness of up to 10 m. The second layer is rather conductive with resistivities ranging between 1 and 2.5 Ωm and a variable thickness of 25-35 m. The third layer extends from approximately 30-800 m and has a resistivity of about 4 Ωm. The fourth layer is again rather conductive with resistivities ranging from 2–3 Ωm and a thickness of 4000-6000 m. The resistivity increase of the terminating half-space is presumably the effect caused by the presence of the defined target formation, which may contain possible hydrocarbon deposits. This assumption is based on a geochemical analysis of several selected oil samples in Azerbaijan (Abrams and Narimanov 1997) that lead to the conclusion that most of the oil indeed originates from similar organic facies which are predicted at this depth interval within the survey area. However, based on the strong resistivity variations within the equivalent models, a direct observation of resistivity and depth of this formation is rather doubtful.

Figure 7 displays the inversion models at station 06 obtained along Profile A using both transmitter positions Tx-N and Tx-W (red and blue, respectively). The comparison between the inversion models of both transmitter positions obtained at one station is used to investigate possible 2D/3D resistivity structures within the study area. However, based on the results shown in Fig. 7, the subsurface resistivity distribution is predominantly 1D. The models are fairly similar throughout the entire depth range, with the exception of the fourth conductive layer. At this depth, the resistivities of the models are somewhat ambivalent. Nevertheless, compared to the surroundings, this layer still represents a rather conductive layer, and thus, no clear evidence of a 2D/3D resistivity structure could be observed within the survey area. This conclusion is based on the comparison at all other stations that

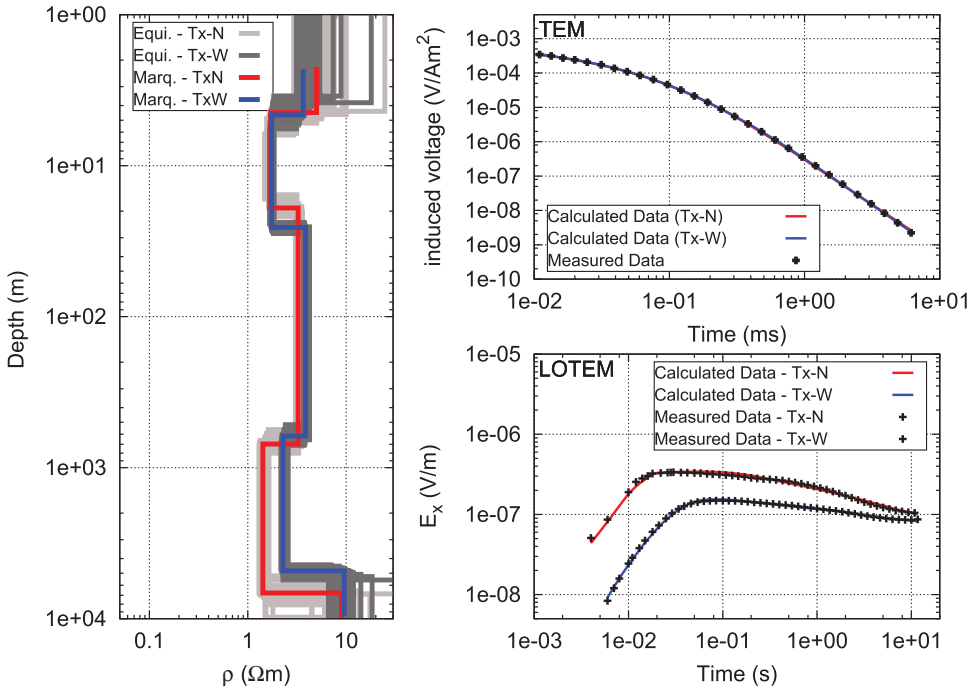

Figure 7 Comparison between the joint Marquardt inversion models obtained at Profile A station 06 from the perpendicular transmitter positions Tx-N (red) and Tx-W (blue). The data fitting of both are displayed on the right.

led to a similar result. Consequently, the use of two perpendicular transmitter positions did not lead to definite evidence that the occurrence of the mud volcanoes within the survey area is related to 2D/3D resistivity structures. Presuming a 1D resistivity distribution for large depths within the survey area is consequently justified.

One common feature of both models in Fig. 7 is the resistivity increase of the terminating half-space at approximately 5000 - 6000 m depth. As mentioned, this effect is presumably caused by the presence of the resistive target formation. However, it is noticeable that the variation of the equivalent models increases, implying a poor resolution of the inversion model at this depth. The assumption that this effect may ultimately be an artefact of inversion also seems reasonable. This issue is treated in further modelling studies (see chapter: Modelling Studies).

All inversion models obtained along Profile A using Tx-N are displayed in Fig. 8. The topography along the profile and receiver station positions are displayed along the top. Station 01 is thereby the northernmost station, and station 07 is the southernmost (Fig. 2). Station 05 is located directly on top of the investigated mud volcano. The inversion models calculated after Occam (green and blue), Marquardt (red), and the equivalent models (grey) are displayed below, labelled 01-07 according to their position along the profile.

When jointly inverting TEM and LOTEM data, each transient appeals to a certain minimum and maximum resolvable depth. Generally, it is safe to say that TEM resolves rather shallow resistivity structures (<130 m), whereas LOTEM resolves deeper ones (>200 m for the study area in Azerbaijan). At an intermediate depth range, both methods may either have a certain degree of resolution or no resolution at all. Hence, despite the general agreement between the individual inversion models of both methods (Fig. 6, black and blue models), it is rather unlikely that they complement each other perfectly. In case of Occam's joint inversion, this may result in oscillations of the resistivity model within this corresponding depth range (see Fig. 8). Although the algorithm generally punishes strong resistivity variations while attempting to fit both data sets simultaneously, it was noticeable that oscillations of the resistivity model occurred at this intermediate depth range at nearly all stations (01, 05, 06, and 07). On the other hand, the individual inversion models show no sign of this behaviour. Consequently, we interpret these oscillations as artefacts of joint inversion and not as actual resistivity variations. Furthermore, it was observable that the oscillation amplitude could be dampened by introducing the CF into the inversion. Especially in case of Marquardt inversion, this was necessary because, otherwise, a further "imaginary layer" would have to be introduced to compensate the resistivity discontinuity.

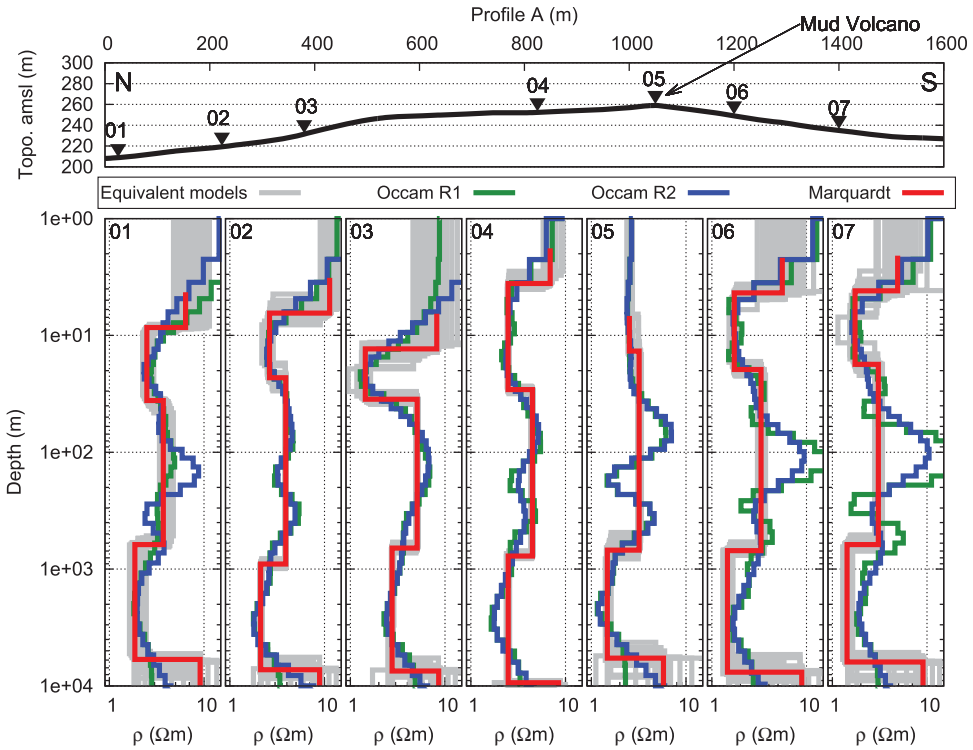

Figure 8 The top image displays the topography along the profile and the receiver positions. The bottom images show 1D joint Occam (green and blue), Marquardt (red) and Monte-Carlo (grey) inversion models of Profile-A utilising the northern transmitter. The inversion models are arranged according to their positions along the profile. Starting from left (north) to right (south), 01 to 07.

Generally, all inversion models along the profile are fairly similar. Apparent is the interrupted resistive overburden at the mud volcano (station 05). This effect is presumably caused by the increased fluid content of the overburden and presence of shallow mud chambers in the vicinity of the mud volcano. Furthermore, the upper boundary of the third layer seems to have an anticline structure with its maximum at the mud volcano. For deeper regions, the 1D joint inversion models show no indication of a possible 2D resistivity structure, i.e., mud plume or fault structure, along the profile. Considering the variations of the equivalent models, the resistivity distribution of the subsurface at large depths (>200 m) is predominantly 1D since a clear distinction between inversion models of successive stations is not possible. For shallower depths, the applied TEM method could clearly distinguish the location of the mud volcano due to the high resistivity contrast of approximately 1:10 to the overburden.

Considering that we obtain an approximate resistivity value of the migrating mud at shallow depths in the vicinity of the mud volcano, we assume that it is also rather conductive at great depths. However, the application of EM methods is only justified if the resistivity of the target object differs significantly from the surrounding media. This is not the case here, and therefore, it is probable that a 2D/3D structure expected to have a rather low resistivity indeed exists within the study area but is not apparent from the EM methods due to the low resistivity contrast with the surrounding media. Also, due to the large offsets applied in the LOTEM measurements, the method averages over a larger volume of subsurface, resulting in a less focused sensitivity distribution. Small resistivity structures, i.e., mud plumes, may therefore be invisible.

The resistivity increase of the terminating half-space is visible in all joint inversion models along the profile. However, similar to before, the resistivity variations of the equivalent models imply that the resistivity possesses a rather poor resolution. This suspicion is validated by the values of the model parameter importance calculated after Menke (1984) displayed in Fig. 9(b,c). The resistivity importances displayed in Fig. 9(b) of the terminating half-space are close to zero for all stations implying a poor resolution. Based on these observations, the presence of a resistive terminating half-space is not confirmed. This conclusion is supported by the eigenparameter (EP) analysis (Jupp and Vozoff 1975b) shown in Fig. 9(d), where all EP values are nearly equal to 0 for $log\rho_5$. However, considering the importances of the fourth layer and the EP9, an indirect observation of the resistivity increase seems feasible. The model parameter importances, in addition to EP9, indicate that the lower boundary and thickness of the

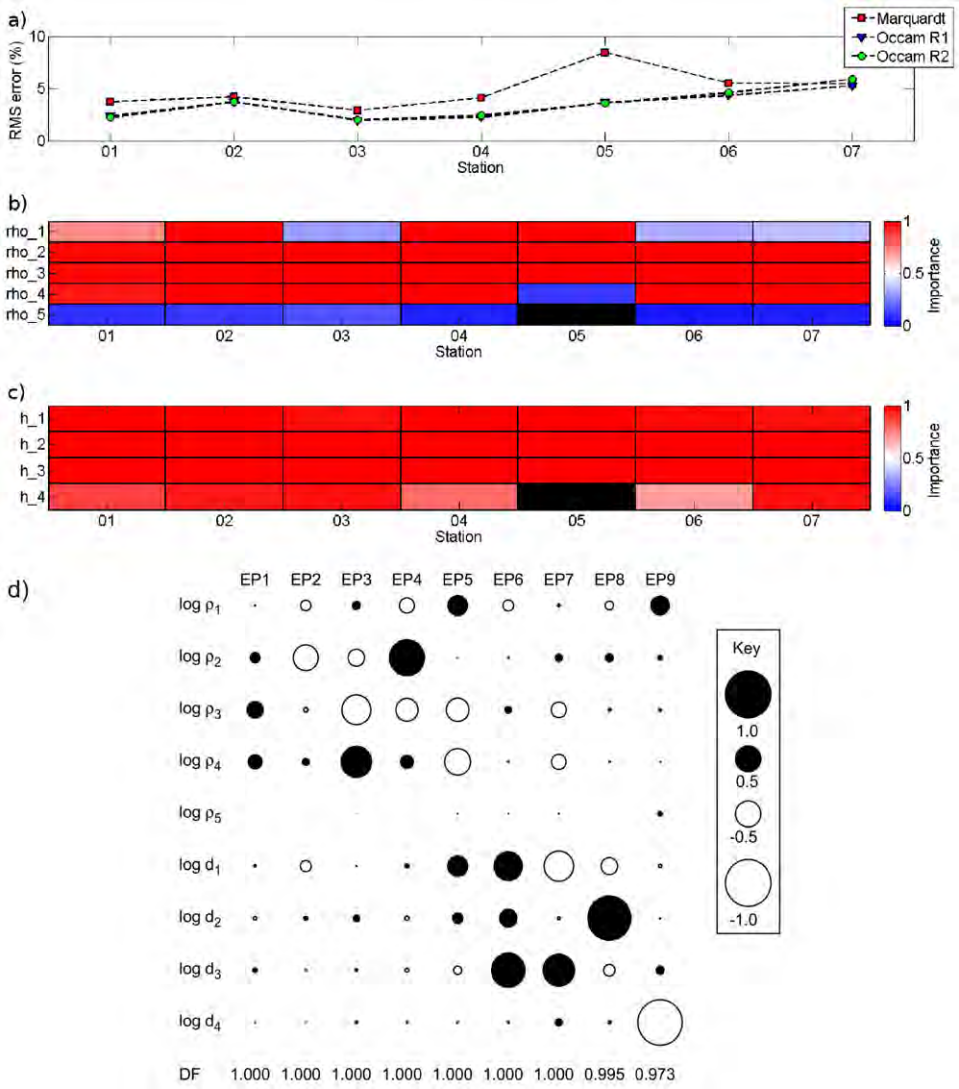

Figure 9 (a) RMS-error of the inversion models at all stations along the profile. (b) and (c) Model parameter importances corresponding to transmitter TxN are displayed (rho_i : resistivity; h_i: depth). Each importance is represented by a single block of constant colour depending on the importance value of the model parameter. They are arranged according to their position along the profile and depth underneath the surface. Note that the model of station 05 possesses one layer less due to the absence of the resistive overburden at the mud volcano. (d) Eigenparameters (EPs) and Damping Factors (DF) at the 1.25 percent level for the inversion model obtained at station 01.

conductive fourth layer are well resolved. Hence, concluding that the presence of the resistive terminating half-space can only be proven based on the presumption that the above lying conductive layer ends at a depth of 5000–7000 m, an additional modelling study seems inevitable to further investigate this issue.

MODELLING STUDIES

The 1D joint inversion models suggest a quasi-horizontal layering of the subsurface. The differences between successive inversion models along the profile are generally justified within the variability of the equivalent models. Furthermore, the terminating half-space at a depth of 5000 m to 6000 m is characterised by a resistivity increase for all inversion models along the profile. However, the variability of the equivalent models and, in addition, the model parameter importances and EPs suggest that the resistivity of the terminating half-space is not resolved. Therefore, additional 1D and 2D modelling studies were performed to examine the late-time transient behaviour for a given subsurface resistivity distribution.

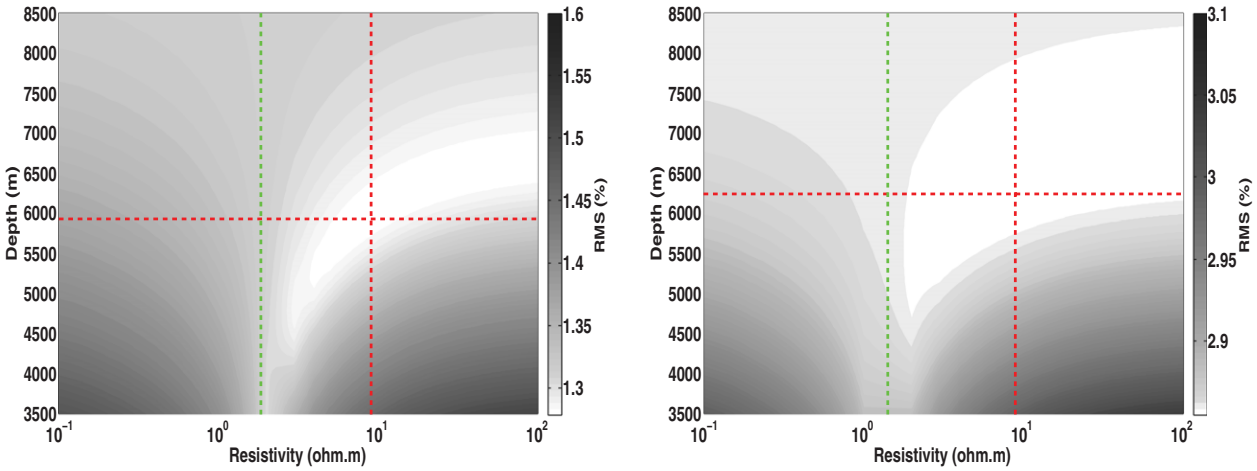

Figure 10 One dimensional modelling study at station 01 (left) and station 07 (right) using LOTEM Ex data. The RMS values are displayed as contours of varying depth and resistivity of the terminating half-space.

1D Modelling Study

To analyse the influence of the terminating half-space on the measured LOTEM Ex transients, additional 1D modelling studies were performed. The resistivity and depth of the terminating half-space were varied for each best-fit Marquardt model along Profile A. Subsequently, the RMS errors of the late times (>1 s) were plotted as a function of resistivity and depth. The results for stations 01 and 07 are displayed in Fig. 10. The red horizontal and vertical lines represent the depth and resistivity of the terminating half-space from best-fit Marquardt model, respectively. The vertical green line represents the resistivity of the fourth layer (e.g., approximately 2 Ωm, see Fig. 8) and is thought as a reference for easier interpretation.

The misfit maps of both stations tend to show that the measured data are best explained by a resistive terminating half-space. The RMS error generally increases for all corresponding depths if a conductive (<2 Ωm) terminating half-space was present. Adversely, a minimum RMS value is reached for a resistive terminating half-space located at a depth greater than 4500 m, depending on the resistivity value. This effect is especially prominent at station 01, whereas it is more questionable at station 07. Also, the modelling study seems quite ambiguous since the resistivity and depth of the terminating half-space seem to be strongly coupled and are not well resolved due to the large range of equivalent models (white area). Nevertheless, it seems at least reasonable that the lower half-space is more resistive than the overlying conductive layer, even if there is ambiguity in its resistivity and depth. Its presence can generally be assumed based on the measured LOTEM data, but additional information, i.e., seismic or borehole data, is needed for a distinct interpretation regarding depth and resistivity.

2D Modelling of LOTEM Ex Transients

To counteract the ambiguity of the 1D modelling study, we attempted to perform a similar investigation by deriving a 2D resistivity model satisfying all measured LOTEM Ex transients simultaneously. It should be mentioned that the TEM transients were not considered for this study. All 2D modelling studies were performed utilising the 3D forward code sldmem3t (Druskin and Knizhnerman 1994).

To find the best-fit model, a modified Hedgehog method was applied (Keilis-Borok and Yanovskaja 1967). The general strategy stipulates that model parameters are defined from the 1D Marquardt inversion models and are varied within a certain interval. The applied procedure varies the model parameters p_i in finite steps Δp_i between a minimum value p_{min} and a maximum value p_{max}. Synthetic data are calculated for all possible parameter combinations and subsequently compared with the measured data. The minimum fitting is consequently obtained by systematically searching through the model parameter space. Unfortunately, this procedure leads to a large number of models and is computationally expensive for a given number of model parameters and small step sizes. This limitation restricts the extent of the 2D modelling procedure of the Azerbaijan project. For example, the 1D joint inversion Marquardt model consists of five layers (e.g., Fig. 8) meaning nine model parameters are to be determined: five resistivities and four layer thicknesses. Splitting the model space of each parameter into four steps would result in 4^9 forward

Table 1 Summary of the 2D modelling procedure. The resistivities of the shallow layers are averaged and fixed, whereas the resistivities of the deeper layers are varied within the interval displayed. The layer boundaries of the shallow layers are interpolated along the profile and not varied during the study. The lower boundary depths (h_i) of layers 3 and 4 are varied.

Layer	Parameter	Value
1	ρ_1 north of MV	9 Ωm (fixed)
	ρ_1 south of MV	4.8 Ωm (fixed)
	h_1	interpolated (fixed)
2	ρ_2	2.15 Ωm (fixed)
	h_2	interpolated (fixed)
3	ρ_3	2 Ωm–5 Ωm
	h_3	600 m–1000 m
4	ρ_4	1.5 Ωm–3.5 Ωm
	h_4	4000 m–8000 m
5	ρ_5	1.5 Ωm–5.5 Ωm

calculations. This is not feasible within an appropriate time frame. Therefore, due to the high computational expense, the assembly of a sufficient modelling procedure was restricted. To consequently limit the extent of the 2D modelling study, shallow regions (<40 m) were grouped into areas with similar resistivities since they are not resolved by the LOTEM Ex data (Fig. 6). The shallow layer boundaries were interpolated along the profile according to the 1D inversion models of TEM. Hence, the nine initial model parameters of the 1D joint inversion were reduced to five: three resistivities and two layer thicknesses. Subsequently, these remaining model parameters were systematically determined by dividing each parameter interval into five steps. The total number of forward calculations reduced to 3125 for each transmitter–receiver configuration. Table 1 summarises the variations of the model parameters for the 2D modelling study.

The best-fit 2D resistivity model of Profile A using the northern transmitter is displayed in Fig. 11. All Ex transients were fitted with a global RMS error of 3.12%. The data fitting at selected stations along Profile A is displayed in Fig. 12. In general, the resistivity distribution is similar to the results of the 1D joint inversion. The terminating half-space has a resistivity of 4 Ωm and starts at a depth of 5000 m, again implying a resistive adjacent half-space. However, as demonstrated by the 1D modelling studies, the resistivity value and depth could also be considerably higher without significantly changing the degree of fitting. Nonetheless, since all LOTEM-Ex transients are best explained by a geological model with a resistive layer at depth, it is the most likely setting.

CONCLUSION

A joint interpretation of measured TEM and LOTEM data was performed to investigate the subsurface resistivity distribution of a mud volcano in the Perekishkul region of Azerbaijan. The subsurface within the study area is generally characterised by relatively low resistivities ranging between 1 Ωm and 10 Ωm. These low resistivities were somewhat problematic and forced long LOTEM recording times. This unconventional time range of the recorded time series of up to 15 s is a novelty. Previous LOTEM measurements performed by the University of Cologne were limited to time-series lengths of only several seconds.

The applied TEM method was highly effective in resolving the shallow resistivity structure of up to approximately 130 m. Due to the high resistivity contrast between the resistive overburden and the conductive mud volcano of approximately 10:1, the lateral extend of the mud volcano could be easily distinguished. In contrast, at large depths, the applied LOTEM method was not able to determine potential fluid migration paths due to the low resistivity contrast to the surrounding media. This does not coincide with the original presumption that the occurrence of mud volcanism is linked to 2D/3D resistivity structures, i.e., a fault or a mud plume. However, this conclusion has to be treated with caution since additional factors are likely to have influenced the results of the LOTEM measurements. These factors can be summarised as follows.

(i) Low resistivities of the subsurface in combination with small resistivity contrasts: Generally, the application of EM methods is justified if the resistivity of the target object differs significantly from the surrounding media. Due to the scarce a priori information of the survey area, the generally low resistivities were not known beforehand. Therefore, it is probable that a 2D/3D structure, expected to have a rather low resistivity, indeed exists within the study area but is invisible for EM methods due to the small resistivity contrast to the surrounding media.

(ii) Large offsets utilised for the LOTEM method in addition to the small spatial extent of the mud volcano: The application of the TEM method indeed proved that the lateral extent of the mud volcano is measurable using EM methods. Due to the large offsets applied for LOTEM, the method averages over a larger volume of subsurface resulting in a less focused sensitivity distribution. Small structures are therefore more likely to be overseen. Hence, future LOTEM field surveys investigating mud volcanoes should be applied on larger objects, such as the Lokbatan mud volcano near Baku.

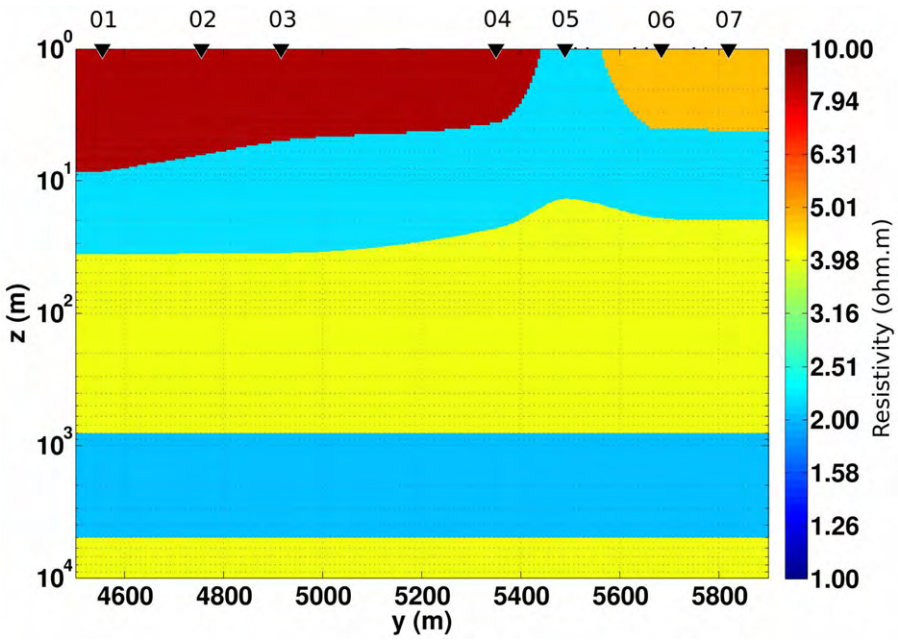

Figure 11 Best-fit model of 3125 forward calculations applying the Hedge-hog method. The positions of the LOTEM Ex stations are marked by black triangles. The mud volcano is situated at station 05.

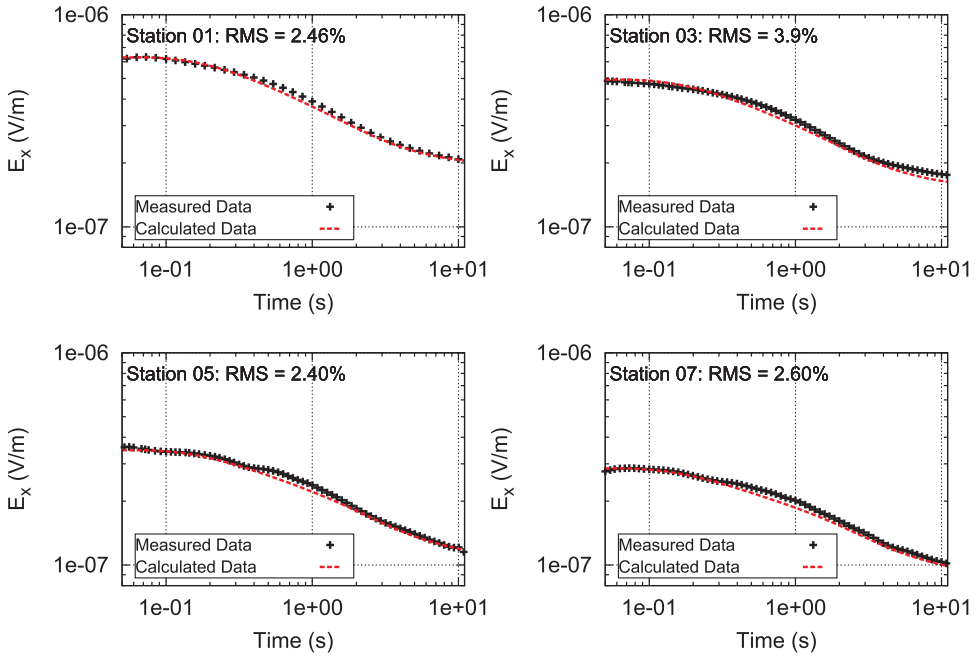

Figure 12 Data fitting of the best-fit 2D resistivity model shown in Fig 11. LOTEM Ex transients at the selected stations 01, 03, 05, and 07 are displayed.

The second aim of the survey was to delineate the depth of a resistivity increase caused by the presence of a hydrocarbon-carrying formation. Indeed, all 1D joint inversion models tend to show a resistive terminating half-space at an approximate depth of 5000-7000 m. However, the model parameter resolution at this depth is very poor, and consequently, the resistivity increase may also be an inversion artefact. Additional 1D/2D modelling studies were performed to investigate the influence

of the terminating half-space on the late-time behaviour of the measured transients. The results of these modelling studies indicated that a resistivity increase is presumably not the result of an inversion artefact but is influenced by the resistive geological formation. However, due to equivalence, the modelling studies also proved that an accurate delineation regarding depth and resistivity of this terminating half-space is not possible. Further geophysical data, i.e., borehole or seismic data, are necessary.

ACKNOWLEDGEMENTS

First and foremost, the authors would like to thank A. Swidinsky, an anonymous reviewer, and associate editor A. T. Basokur for the constructive criticism that substantially improved this publication. Furthermore, they would like to thank Volkswagen Stiftung for the funding of this project in the extent of the program "Zwischen Europa und Orient–Mittelasien/Kaukasus im Fokus der Wissenschaft". Additionally, they would like to acknowledge the partners in Azerbaijan along with all the helpers during the field survey for their great effort. A special thanks goes out to their colleagues K. Lippert, H. Grossbach, and M. Seidel for assisting during the field measurements. Furthermore, they would like to thank KMS Technologies for supporting the LOTEM field measurements with the KMS820 acquisition unit.

REFERENCES

Abrams M.A. and Narimanov A.A. 1997. Geochemical evaluation of hydrocarbons and their potential sources in the western South Caspian depression, Republic of Azerbaijan. *Marine and Petroleum Geology* **14**(4), 451–468.

Aliyev A.A., Guliyev I.S. and Rahmanov R.R. 2009. Catalogue of Mud Volcanoes Eruptions of Azerbaijan *(1810–2007)*, 2nd edn. Nafta Press, Baku, Azerbaijan.

Bohrmann G., Kopf A. and Spiess V. 2006. Vulkane, die Schlamm statt Lava speien. Expedition Erde (336).

Bonini M., Tassi F., Feyzullayev A.A., Aliyev C.S., Capecchiacci F. and Minissale A. 2013. Deep gases discharged from mud volcanoes of Azerbaijan: New geochemical evidence. *Marine and Petroleum Geology* **43**(0), 450–463.

Brunet M.F., Korotaev M., Ershov A.V., Nikishin A.M. 2002. The South Caspian Basin: A review of its evolution from subsidence modelling. *Sedimentary Geology* **156**, 119–148.

Chow J., Chang S. and Yu H. 2006. GPR refelction characteristics and depositional models of mud volcanic sediments – Wushanting mud volcano field, southwestern Taiwan. *Journal of Applied Geophysics* **60**(3–4), 179–200.

Constable S.C., Parker R.L. and Constable C.G. 1987. Occam's inversion: A practical algorithm for generating smooth models from electromagnetic sounding data. *Geophysics* **52**(3), 289–300.

Druskin V.L. and Knizhnerman L.A. 1994. Spectral approach to solving three-dimensional Maxwell's diffusion equations in the time and frequency domains. *Radio Science* **39**, 937–953.

Ellis M., Evans R., Hutchinson D., Hart P., Gardner J. and Hagen R. 2008. Electromagnetic surveying of seafloor mounds in the northern Gulf of Mexico. *Marine and Petroleum Geology* **25**(9), 960–968.

Feyzullayev A.A., Kadirov F.A. and Aliyev C.S. 2005. Mud Volcano Model Resulting from Geophysical and Geochemical Research. *Mud Volcanoes, Geodynamics and Seismicity*.

Fitterman D.V. and Anderson W.L. 1987. Effect of transmitter turn-off time on transient soundings. *Geoexploration* **24**(2), 131–146.

Hanstein T. 1996. Digitale Optimalfilter für LOTEM Daten. In: Baur K., Junge A. (Eds.), *Protokoll über das 16. Kolloquium Elektromagnetische Tiefenforschung*. Deutsche Geophysikalische Gesellschaft.

Helwig S.L., Lange J. and Hanstein T. 2003. Kombination dekonvolvierter Messkurven zu einem langen Transienten. In: Tagungsband der 63. Jahrestagung der Deutschen Geophyikalischen Gesellschaft. Deutsche Geophysikalische Gesellschaft.

Hördt A. 1989. Ein Verfahren zur 'Joint Inversion' angewandt auf Long Offset Transient Electromagnetics and Magnetotellurik. Master's thesis, University of Cologne, Germany.

Hördt A. and Scholl C. 2004. The effect of local distortions on time-domain electromagnetic measurements. *Geophysics* **69**, 87–96.

Hördt A., Jödicke H., Strack K.-M., Vozoff K. and Wolfgram P.A. 1992. Inversion of long-offset TEM soundings near the borehole Münsterland 1, Germany, and comparison with MT measurements. *Geophysical Journal International* **108**(3), 930–940.

Istadi B., Pramono G., Sumintadireja P. and Alem S. 2009. Modelling study of growth and potential geohazard for LUSI mud volcano:*East Java, Indonesia*. *Marine and Petroleum Geology* **25**(9), 1724–1739.

Judd A. 2005a. Gas emissions from mud volcanoes. In: *Mud Volcanoes, Geodynamics and Seismicity*, Vol. **51** (eds. G. Martinelli and B. Panahi) of NATO Science Series, pp. 147-157. Springer, Netherlands. URL

Judd A. 2005b. *Mud Volcanoes, Geodynamics and Seismicity*, pp. 147–157. Springer.

Jupp D.L.B. and Vozoff K. 1975a. Joint Inversion of Geophysical Data. *Geophysical Journal* **42**, 977–991.

Jupp D.L.B. and Vozoff K. 1975b. Stable Iterative Methods for the Inversion of Geophysical Data, *Geophysical Journal* **42**, 957–976.

Kaufman A.A. and Keller G.V. 1983. Frequency and transients soundings. Elsevier, Amsterdam.

Keilis-Borok V.I. and Yanovskaja T.B. 1967. Inverse Problems of Seismology (Structural Reveiw), *Geophysical Journal of the Royal Astronomical Society* (Today: Geophysical Journal International) **13**, 223–234.

Lange J.O. 2003. Joint Inversion von Central-Loop-TEM und Long-Offset-TEM Transienten am Beispiel von Messdaten aus Isreal 2002. Master's thesis, University of Cologne, Germany.

Lerche I., Bagirov F., Nadirov M., Tagiyev M. and Guliyev I.S. 1996. Evolution of the South Caspian Basin: geologic risks and probable hazards. Azerbaijan Academy of Sciences, 580.

Lin M. and Jeng Y. 2010. Application of the VLF-EM method with EEMD to the study of a mud volcano in southern Taiwan. *Geomorphology* **119**(1–2), 97–110.

Lippert K., Tezkan B., Bergers R. and Goldman M. 2012. Erkundung eines Aquifers unter dem Mittelmeer vor der israelischen Küste mit Long Offset Transient Elektromagnetik. In: 72. Jahrestagung der Deutschen Geophysikalischen Gesellschaft.

Marquardt D.W. 1963. An algorithm for least-squares estimation of non-linear parameters. *Journal of the Society for Industrial and Applied Mathematics* **12**, 591–612.

Menke W. 1984. Geophysical Data Analysis: Discrete Inverse Theory. Academic Press, Inc.

Milkov A.V. 2000. Worldwide Distribution of submarine Mud Volcanoes and Associated Gas Hydrates. *Marine Geophysics* **167**, 29–42.

Milkov A.V. 2005. Global Distribution of Mud Volcanoes and their significance in Petroleum Exploration as a source of Methane in the Athmosphere and Hydrosphere and as a Geohazard. *Mud Volcanoes, Geodynamics and Seismicity*. Springer.

Müller M., Hördt A. and Neubauer F.M. 2002. Internal structure of Mount Merapi, Indonesia, derived from long-offset transient electromagnetic data. *Journal of Geophysical Research: Solid Earth* (1978–2012) **107** (B9), ECV 2–1–ECV 2–14.

Nabighian M.N. and Macnae J.C. 1991. Electromagnetic Methods in Applied Geophysics. Time Domain Electromagnetic Prospecting Methods. Society of Exploration Geophysicists.

Newman G.A. 1989. Deep transient electromagnetic soundings with a grounded source over near-surface conductors. *Geophysical Journal* **98**, 587–601.

Planke S., Svensen H., Hovland M., Banks D.A., and Jamtveit B. 2003. Mud and fluid migration in active mud volcanoes in Azerbaijan. *Geo-Marine Letters* **23**, 258–268.

Scholl C. 2005. The influence of multidimensional strucutres on the interpretation of LOTEM data with one-dimensional models and the application to data from Israel. PhD thesis, University of Cologne, Germany.

Scholte K.H. 2005. Hyperspectral Remote Sensing and Mud Volcanism in Azerbaijan. PhD thesis, Delft University of Technology, The Netherlands.

Stephan A., Schniggenfitting H. and Strack K.-M. 1991. Long-Offset Transient EM Sounding North of the Rhine-Ruhr Coal District, Germany. *Geophysical Prospecting* **39**(4), 505–525.

Stewart S.A. and Davies R.J. 2006. Structure and emplacement of mud volcano systems in the South Caspian Basin. *AAPG Bulletin* **90**(5), 771–786.

Strack K.M. 1992. Exploration with Deep Transient Electromagnetics. Elsevier.

Swidinsky A., Hölz S. and Jegen M. 2013. Rapid resistivity imaging using a transient marine CSEM survey with two transmitter polarisations. In: EAGE conference. EAGE.

The CGIAR Consortium for Spatial Information, 2012. SRTM 90m Digital Elevation Data.

Ward S. and Hohmann D.L.B. 1988. Electromagnetic Theory for Geophysical Applications. Vol. 1. Electromagnetic Methods in Applied Geophysics, Society of Exploration Geophysics, Ch. 1.